HHS Public Access

Author manuscript

Cell Rep. Author manuscript; available in PMC 2022 October 10.

Published in final edited form as:

Cell Rep. 2022 July 05; 40(1): 111035. doi:10.1016/j.celrep.2022.111035.

Diverging regulation of Bach2 protein and RNA expression determine cell fate in early B-cell response

Qianwen Hu[1,#], **Tingting Xu**[1,#], **Min Zhang**[2], **Heng Zhang**[1], **Yongbo Liu**[1], **Hua-bing Li**[1], **Chiqi Chen**[3], **Junke Zheng**[3], **Zhen Zhang**[2], **Fubin Li**[1], **Nan Shen**[4], **Wenqian Zhang**[1,*], **Ari Melnick**[5,*], **Chuanxin Huang**[1,3,6,*]

[1]Center for Immune-Related Diseases at Shanghai Institute of Immunology, Ruijin Hospital, Shanghai Jiao Tong University School of Medicine, Shanghai, China

[2]Shanghai Pediatric Congenital Heart Disease Institute and Pediatric Translational Medicine Institute, Shanghai Children's Medical Center, Shanghai Jiao Tong University School of Medicine, Shanghai, China

[3]Key Laboratory of Cell Differentiation and Apoptosis of Chinese Ministry of Education, Faculty of Basic Medicine, Shanghai Jiao Tong University School of Medicine, Shanghai, China

[4]Shanghai Institute of Rheumatology, Renji Hospital, Shanghai Jiao Tong University School of Medicine, Shanghai, China

[5]Division of Hematology/Oncology, Department of Medicine, Weill Cornell Medicine, Cornell University, New York, USA

[6]Lead Contact

Summary:

During the early phase of primary humoral responses, activated B cells can differentiate into different types of effector cells, dependent on B cell receptor affinity for antigen. However, the pivotal transcription factors governing these processes remain to be elucidated. Here, we show that transcription factor Bach2 protein in activated B cells is transiently induced by affinity-related signals and mTORC1-dependent translation to restrain their expansion and differentiation into plasma cells while promoting memory and germinal center (GC) B cell fates. Affinity-related signals also down-regulates *Bach2* mRNA expression in activated B cells and their descendant memory B cells. Sustained and higher concentrations of Bach2 antagonize the GC fate. Repression of Bach2 in memory B cells predisposes their cell-fate choices upon memory recall. Our study reveals that differential dynamics of Bach2 protein and transcripts in activated B cells controls their cell-fate outcomes and imprints the fates of their descendant effector cells.

*Correspondence: huangcx@shsmu.edu.cn (C.H.), amm2014@med.cornell.edu (A.M.) or dzzhangwenqian@126.com (W.Z.).
#These authors contributed equally to this study

Author Contributions

Q.H. and T.X. performed the most experiments and interpreted the data. M.Z., H.Z. and Z.Z analyzed the high-throughput sequencing data. Y. L., C.C. and HB. L. performed and analyzed polysome profiling. F.L., J.Z. and N.S. helped to interpret data and edit the manuscript. C.H., A.M and W.Z. supervised the project and wrote the paper.

Declaration of Interests

The authors declare no competing interests.

Keywords

Bach2; plasma; memory; germinal center; activated B cells

Introduction

After immunization with T cell-dependent (TD) antigens, antigen-specific B-cells are activated by the binding of antigens to B cell antigen receptor (BCR) and migrate to the periphery of B cell follicles and interfollicular zones of secondary lymphoid organs, where they form cognate interactions with T follicular helper (Tfh) cells within 1-3 days (Cyster and Allen, 2019; De Silva and Klein, 2015). Antigen binding alone initiates a cascade of signaling events that are necessary but not sufficient to induce B cell expansion and further differentiation (Turner et al., 2020). With the help of T cells, antigen-engaged activated B cells rapidly proliferate and differentiate into three types of effector cells: extrafollicular short-lived plasma cells (PCs) secreting low-affinity antibodies, follicular germinal center (GC) B-cells and early GC-independent memory B cells (Cyster and Allen, 2019; Dhenni and Phan, 2020; Kurosaki et al., 2015; Taylor et al., 2012; Taylor et al., 2015). GC-independent memory B cells are dominantly IgM^+ and $CD80^-$ population, which preferentially participate in secondary GCs upon secondary immunization (Gitlin et al., 2016; Pape et al., 2011; Taylor et al., 2012; Zuccarino-Catania et al., 2014). Understanding molecular pathways controlling these processes are critical for vaccine development, interpretation of vaccine efficacy and the treatment for autoimmune diseases (Elsner and Shlomchik, 2020).

At the pre-GC stage, the expansion of activated B cells and subsequent differentiation into diversified effector cells are largely controlled by the affinity of BCRs for their cognate antigens and require the help of T cells (Chan et al., 2009; Paus et al., 2006; Schwickert et al., 2011; Shih et al., 2002). High-affinity crosslinking drives rapid B cell expansion and predisposes them to differentiate towards PCs (Chan et al., 2009; Paus et al., 2006; Phan et al., 2006). B cells with intermediate BCR affinity preferentially enter the GC pathway, whereas clones with weaker antigen reactivity are supposed to be directed to the memory pools (Kaji et al., 2012; Taylor et al., 2015). Higher BCR affinity is likely to induce stronger BCR signals and subsequently stronger T cell help in the form of CD40L and cytokines, such as interleukin-4 (IL-4) and IL-21(Ise and Kurosaki, 2019; Victora and Nussenzweig, 2012). T cell help and CD40 engagement are limited to B cells that can present cognate antigens via MHCII, thus allowing for a dynamic affinity threshold to be imposed on antigen-binding B cells (Schwickert et al., 2011). Affinity-based signals have been demonstrated to regulate the expression and activity of key “fate-determining” transcription factors to orchestrate cell-fate choices. Either BCR or CD40 signals can induce the expression of the transcription factor IRF4, and the intensity of their strength scales with IRF4 concentrations (Luo et al., 2018; Sciammas et al., 2006). IRF4 is critically involved in the fate decision of activated B cells by regulating the expression of two counter-antagonistic cell fate determinants, Bcl6 and Blimp1 (encoded by *Prdm1*) (Ochiai et al., 2013; Sciammas et al., 2006). Similar to GC B cells, memory B cells originate from activated B cells with

lower BCR affinity. However, the essential transcription factors that direct memory B cell differentiation versus other cell fates at the pre-GC stage remain poorly understood.

The transcription factor Bach2 is highly expressed within GC B cells and regulates the GC program via direct suppression of *Prdm1* (Huang et al., 2014; Muto et al., 2010; Muto et al., 2004). Repression of Bach2 expression in GC-derived $IgG1^+$ memory B cells has been shown to predispose them to differentiate into plasma cells upon memory recall (Kometani et al., 2013). Bach2 is also required for the formation of GC-dependent memory B cells (Shinnakasu et al., 2016). Lower-affinity light zone GC B cells, which are a memory-prone population, express higher levels of *Bach2* transcripts (Shinnakasu et al., 2016). However, it remains unclear whether increased *Bach2* transcripts in this population are an indicator of BCR affinity or actually contribute to selection into the memory pool. It is also unknown whether Bach2 protein is expressed by these cells in the similar model as its transcript. Paradoxically, GC B cells express more *Bach2* transcripts than memory B cells (Wang et al., 2017). More recently, we showed that human lymphoma-derived TBL1XR1 mutations skew the humoral immune response towards producing memory B cells by increasing the transcriptional activity of *Bach2* (Venturutti et al., 2020). These results suggest that precise Bach2 expression kinetics might influence the fate decision of GC B cells in the light zone. Finally, the precise functions of Bach2 in alternative cell-fate decisions during the early phase of primary humoral responses have never been explored. Herein, we explore affinity-based precise Bach2 protein and mRNA expression kinetics in various B subsets during this early phase and its impact on alternative cell-fate decisions.

Results

Bach2 restrains activated B cell expansion and PC differentiation

To trace the dynamics of very rare antigen-engaged B cells in vivo at the pre-GC stage, we performed adoptive transfer experiments using B1-8^{hi} B cells in which the VH186.2 heavy chain is knocked into the heavy chain locus and recognizes hapten 4-hydroxy-3-nitrophenylacetyl (NP) when paired with endogenous λ light chains (Shih et al., 2002). Transferred NP-specific B cells were activated and underwent rapid expansion in the first 3 days after immunization with NP-OVA (Figures S1A and S1B). $CD38^+GL7^-$ memory B cells and $CD19^+CD138^+$ plasmablasts could be detected as early as day 2, and the majority of transferred NP^+ cells became $CD38^+GL7^+$ active precursors on day 3 (Figure S1C). Starting on day 3, the donor NP-specific B cells gave rise to bursts of various effector subsets comprising $CD19^{lo/-}CD138^+$ antibody-secreting PCs, $CD19^+CD38^-GL7^+$ GC B cells and $CD19^+CD38^+GL7^-$ memory B cells (Figure S1C), as described previously (Taylor et al., 2012; Taylor et al., 2015). The identity of PCs and GC B cells was further confirmed by assessment of the lineage-specific transcription factors IRF4 and Bcl6, respectively (Figure S1D).

To analysis the roles of Bach2 on alternative cell-fate choices at the pre-GC stage, we analyzed the differentiation of transferred B1-8^{hi} wild-type and *Bach2*-deficient cells under competitive conditions (Figure 1A). Although donor non-NP-binding *Bach2*-deficient B cells showed a slight reduction in homing to the spleens, they had no competitive disadvantage when compared to their wild-type counterparts after immunization (Figure

1A). However, the ratio between *Bach2*-deficient and wild-type compartments among donor NP-specific B cells was significantly increased on days 2-3 after immunization (Figure 1A). Interestingly, this increase rapidly declined after day 3, and *Bach2*-deficient NP-specific B cells showed an obvious competitive disadvantage on day 7 (Figure 1A). After contact with cognate T cells, activated B cells undergo rapid expansion in the first 3 days after immunization, and then produce a burst of effector cell differentiation (Figure S1C). The BrdU pulse labeling experiments demonstrated that more *Bach2*-deficient NP-specific activated B cells were in the S phase on day 2 after immunization (Figure 1B). Although *Bach2*-deficient B cells were prone to die upon BCR activation in vitro, they exhibited activated caspase-3 expression similar to that of their wild-type counterparts in vivo on day 2 after immunization (Figure S2A). *Bach2*-deficient memory B cells and active precursors underwent more rounds of division than their wild-type counterparts on day 3, as indicated by increased CFSE dilution (Figure 1C), indicating that Bach2 constrains B cell proliferation prior to full differentiation into effector cells. We next asked whether *Bach2* deficiency disrupts the differentiation of effector cells. *Bach2* deficiency markedly accelerated the expansion and differentiation of $CD19^{-}CD138^{+}$ PCs on day 3, and this tendency obviously declined on day 7 (Figure 1D). This result is probably because early extrafollicular PCs are short-lived and die several days after birth. The generation of *Bach2*-deficient $CD38^{+}GL7^{-}$ memory and $CD38^{+}GL7^{+}$ active precursors tended to decrease on day 3 (Figure 1D). Strikingly, the *Bach2*-deficient compartment almost lost $CD38^{+}GL7^{™}$ memory and $CD38^{-}GL7^{+}$ GC B cells and their precursors under competitive conditions on day 7 (Figure 1D). Moreover, *Bach2* deficiency markedly promoted the generation of $IRF4^{+}$ cells on day 3 and suppressed the formation of $Bcl6^{+}$ cells on day 7 (Figure S2B). In a noncompetitive environment, donor *Bach2*-deficient NP^{+} cells generated a greater percentage of PCs with lower percentages of memory and GC B cells (Figure S2C). Therefore, Bach2 prevents expedited PC differentiation while facilitating memory and GC cell fate at the pre-GC stage.

Bach2-deficient activated B cells enforce the transcriptional program of PCs

To gain mechanistic insight into the suppressive effects of Bach2 on PC differentiation, wild-type and *Bach2*-deficient $GL7^{+}CD38^{+}$ activated NP-specific B cells were sorted on day 2 after immunization and subjected to transcriptional profile analysis. In total, we detected 706 upregulated genes and 436 downregulated genes (FDR<0.01, fold change>2) in *Bach2*-deficient activated B cells compared to wild-type control cells (Figure 2A). Notably, PC-specific transcription factors, including *Prdm1* and *Irf4*, were markedly upregulated in *Bach2*-deficient cells. Consistent with a previous report (Muto et al., 2004), *Aicda* was also downregulated in these cells. We selected representative genes that were upregulated in PCs (FDR<0.01, fold change>4) relative to memory or GC B cells for gene set enrichment analysis (GSEA). This analysis revealed that two PC-upregulated gene signatures were significantly overexpressed in *Bach2*-deficient activated B cells (Figure 2B). Gene ontology analysis further showed that *Bach2*-deficient activated B cells upregulated gene signatures associated with the endoplasmic reticulum (ER) remodeling and unfolded protein response (UPR) and downregulated gene sets related to B cell activation and proliferation (Figure S3A). In particular, the expression of IRE1α/XBP1, a key axis of the UPR pathway, was enhanced in *Bach2*-deficient activated B cells. The IRE1α-XBP1 axis is essential for ER

expansion and plays a central role in the development and antibody production of PCs (Benhamron et al., 2014; Iwakoshi et al., 2003). A recent study showed that activated B cells up-regulate ER remodeling- and UPR-genes to prepare for antibody production and secretion when differentiating towards PCs (Gaudette et al., 2020). These results suggest that the transcriptional profile of *Bach2*-deficient activated B cells has switched towards that of PCs. By analyzing published BACH2 ChIP-seq data in human activated B cells (Hipp et al., 2017), we identified approximately 12,968 genomic regions bound by BACH2. We performed LiftOver analysis with human BACH2 binding peaks and the mouse genome and obtained 6,844 conserved Bach2 binding peaks. A total of 131 out of 706 upregulated genes, including *Irf4* and *Prdm1*, in *Bach2*-deficient cells contained at least one Bach2 binding site within 5 kb of their transcription start site (TSS) (Figures 2C and S3B), indicating that they are direct targets of Bach2. Analysis of the enriched motif of these binding sites at 131 genes identified the Bach2 consensus binding motif, which embeds the canonical AP-1 motif (Figure 2C).

We and other reported that Bach2 directly binds to the promoter region of *Prdm1* to repress its transcription in human and murine B cells (Huang et al., 2014; Ochiai et al., 2008). ChIP-QPCR confirmed the enrichment of Bach2 at the predicted Bach2-binding site at the promoter of *Irf4* gene in activated murine B cells (Figure S3C). Moreover, up-regulation of *Irf4* mRNA abundance occurred in activated *Bach2*-deficient B cells as early as 16 h after BCR ligation, a time-point before the onset of PCs differentiation and Blimp1 up-regulation (Figures S3D and S3E). These findings collectively suggest that Bach2 is capable to directly repress the transcription of *Irf4* in B cells.

The c-Fos/AP-1 transcription factors are activated upon B cell activation, and required for B cell proliferation and PC differentiation in part by promoting IRF4 and Blimp1 expression (Ohkubo et al., 2005). Treatment with T-5224, a specific inhibitor of c-Fos/AP-1 transcription factors that inhibits DNA binding activity, significantly impaired PC differentiation and cell division in the absence of *Bach2* (Figures 2D and 2E). We reason that Bach2 constrains B cell expansion and PC differentiation in part by antagonizing the transcription activity of c-Fos/AP-1 transcription factors.

Bach2 represses the *Irf4-Prdm1* loop to enforce memory and GC B cell fates

Starting from day 3 after immunization, active precursors gave rise to burst of different types of effector subsets (Figure S1C). *Bach2*-deficient active precursors contained a higher proportion of Blimp1^{+}IRF4^{hi} PC-prone cells than their wild-type counterparts on day 3 (Figure 3A). Furthermore, in adoptive transfer experiments *Bach2*-deficient active precursors displayed a higher propensity to differentiate into PCs at the expense of memory and GC B cells (Figure 3B). These results collectively suggest that *Bach2* deficiency induces the generation of Blimp1^{+}IRF4^{hi} PC-prone active precursors to prevent memory and GC B cells differentiation. Blimp1 and IRF4 forms a reciprocal transcription regulatory loop to initiate PC differentiation and both are essential for the generation of PCs (Sciammas et al., 2011; Sciammas et al., 2006; Shapiro-Shelef and Calame, 2005; Tellier et al., 2016). Reduction of either Blimp1 or IRF4 is able to damage the loop to inhibit PC differentiation. To examine whether *Bach2* deficiency prevents memory and GC B cell fates by activating

the *Irf4-Prdm1* loop, we performed adoptive transfer using *Bach2*-deficient B1-8^{hi} cells expressing scramble (scr), shRNA against *Prdm1* (sh*Prmd1*) or *Irf4* (sh*If4*). Either *Prdm1* or *Irf4* knockdown markedly reduced the fractions of PCs, accompanied with increased proportions of memory and GC B cells among donor NP-specific B cells (Figure 3C). Thus, Bach2 restrains the *Irf4-Prdm1* loop to allow memory and GC B cell differentiation.

BCR stimulation represses Bach2 transcription, but increases its protein abundance

Having demonstrated that the importance of Bach2 expression in the B cell-fate decision at the pre-GC stage, we sought to understand how Bach2 expression is regulated. Consistent with previous reports (Kometani et al., 2013; Shinnakasu et al., 2016), BCR stimulation reduced *Bach2* mRNA abundance in B cells in a dose-dependent manner, and this effect occurred as early as 6 h after treatment (Figure 4A). To our surprise, BCR stimulation dramatically upregulated Bach2 protein expression 24 h after treatment (Figure 4B). IRF4 upregulation occurred as early as 3 h after treatment (Figure 4B). Intriguingly, upregulation of either Bach2 or IRF4 protein was proportional to the concentrations of anti-IgM antibody at 24 h after treatment (Figure 4C). Similar results were observed in B cells stimulated with anti-CD40 antibody, the Toll-like receptor 4 ligand lipopolysaccharide (LPS) and the Toll-like receptor 9 ligand CpG oligonucleotides (Figure 4D). Interestingly, coactivation of BCR and CD40 signaling synergistically induced Bach2 protein expression and downregulated its mRNA abundance (Figure 4D). These results indicate that Bach2 protein and mRNA levels are controlled by a range of B cell stimulators, which can result in opposite directions of regulation.

By analyzing published chromatin immunoprecipitation sequencing (ChIP-seq) data from our previous study and others (Hipp et al., 2017; Huang et al., 2014; Ochiai et al., 2013), we found that IRF4 and BACH2 bind to the *Bach2* gene (Figure 4E). Upon BCR activation either *Irf4*- or *Bach2*-deficient B cells reduced *Bach2* transcripts but to a lesser extent than did their wild-type counterparts (Figure 4F), suggesting that IRF4 and Bach2 directly suppress *Bach2* transcription. Of note, to assess *Bach2* transcription in *Bach2*-deficient cells, primers were designed to amplify the exon 1 of *Bach2*, which is not deleted in these cells. In conclusion, BCR stimulation increases Bach2 and IRF4 protein expression which in turn inhibits Bach2 transcription.

Differential expression of *Bach2* mRNA in activated B cells and various effector subsets

To monitor the kinetics of *Bach2* mRNA expression in vivo, we constructed a Bach2-GFP (*Bach2*^{EGFP}) mRNA reporter mouse (Figures S4A and S4B). On day 2 after immunization, the expression of the *Bach2* mRNA reporter in memory and activated B cells remained largely unchanged, and its levels were obviously attenuated in CD19^{+}CD138^{+} plasmablasts, compared to non-NP binding donor B cells (Figure 5A). On day 5, CD38^{+}GL7^{-} memory B cells and CD38^{+}GL7^{+} active precursors maintained lower but modest levels of *Bach2* mRNA reporter than naïve NP^{-} B cells (Figure 5B). CD19^{-}CD138^{+} PCs had almost lost expression of the *Bach2* mRNA reporter, whereas CD38^{-}GL7^{+} GC B cells had largely restored their expression to levels similar to those of naïve NP^{-} B cells (Figure 5B). The differential amounts of *Bach2* transcripts in various effector subsets were further validated

by analyzing the transcriptional profiles of the cells isolated 5 days post-immunization (Figure 5C).

$CD19^+CD38^+GL7^+$ active precursors are heterogenous populations comprising various progenitors for PCs, memory and GC B cells (Taylor et al., 2012; Taylor et al., 2015). We next analyzed the kinetics of *Bach2* mRNA expression in various precursor subsets. The chemokine receptor CCR6 marks memory B precursors in both mouse and human GCs (Suan et al., 2017a). Fully differentiated PCs and GC B cells shut down CCR6 expression on day 5 (Figure 5D), suggesting that they originate from $CCR6^-$ active precursors. Based on CCR6 and CD138 expression, $CD19^+GL7^+$ $CD38^+$ active precursors on day 3 and day 5 were classified into three subsets: $CCR6^-CD138^+$ plasmablasts, $CCR6^-CD138^-$ and $CCR6^+CD138^-$ (Figure 5E). $CCR6^-CD138^-$ active precursors did not express Bcl6 on day 3 after immunization, but on day 5, ~40% of them gained Bcl6 expression, a hallmark of GC B cells (Figure 5E). Bcl6 protein was not expressed by $CCR6^+CD138^-$ active precursors on either day 3 or day 5 (Figure 5E). These results collectively indicate that $CCR6^-CD138^-$ and $CCR6^+CD138^-$ populations can be considered GC and memory precursors, respectively. As expected, $CCR6^-CD138^+$ plasmablasts expressed the lowest amounts of *Bach2* mRNA reporter (Figure 5F). Intriguingly, $CCR6^-CD138^-$ GC precursors expressed lower levels of *Bach2* mRNA reporter than $CCR6^+CD138^-$ memory precursors on day 3 post-immunization; however, this expression feature was reversed on day 5 (Figure 5F). These results indicate that activated B cells with intermediate *Bach2* transcript levels preferentially differentiate into early GC precursors, which gradually restore *Bach2* transcription when differentiating into GC B cells.

Dynamics of Bach2 protein in activated B cells and various effector subsets

The above results indicate that BCR activation promotes Bach2 protein expression at the post-transcriptional levels (Figures 4A–D). The 5’ untranslated region (UTR) of *Bach2* contains GC-rich complex secondary structures and has a predicted ΔG value of −235 (Figure S5A), suggesting a cap-dependent translational control of Bach2 protein. Antigen binding, as well as other B cell stimulators such as CD40 engagement, activates the extracellular-signal-regulated kinase (ERK) and phosphoinositide 3-kinase (PI3-kinase)/AKT pathways to stimulate cap-dependent translation via mechanistic target of rapamycin complex 1 (mTORC1) (Luo et al., 2018; Reth and Wienands, 1997). mTORC1 stimulates the p70S6K/ eIF4A axis to induce cap-complex formation and translation initiation, especially for genes harboring complex secondary structures in 5’ UTRs. BCR stimulation-induced Bach2 protein up-regulation was potently blocked by treatment of inhibitors for ERK, AKT or mTORC1 (Figure 6A). Silvestrol, a pharmacological inhibitor of eIF4A (Wolfe et al., 2014), exhibited the similar activity (Figure 6A). Interestingly, other B cell stimulators including CpG, CD40 and LPS up-regulated Bach2 protein levels via mTORC1 (Figure 6B). We further observed enhanced loading of *Bach2* mRNA in the higher molecular weight polysomal fractions upon BCR activation, which was suppressed by silvestrol treatment (Figure 6C). To evaluate the direct contribution of the 5’ UTR of *Bach2* to protein translation, we cloned it into a dual fluorescence retroviral reporter construct (Figure S5B). In this reporter construct, the mCherry gene was placed under the control of the MSCV promoter and fused to the 5’ UTR sequence of *Bach2.* The transcription of the

internal control GFP was also controlled by the MSCV promoter, but its translation was controlled by the eIF4A-independent IRES element. B cells were infected with retrovirus expressing these reporter constructs, and the expression of GFP and mCherry was measured. After normalization to GFP, the *Bach2* 5' UTR repressed the expression of mCherry protein by 4-fold (Figures S5C and S5D). As retroviral transduction requires stimulated B cells, infected B cells harbored active BCR signaling, partially unleashing the *Bach2* 5' UTR. We observed that silvestrol treatment significantly diminished mCherry protein expression, but not GFP, in the presence of the *Bach2* 5' UTR (Figures S5C and S5E). In contrast, silvestrol treatment had no effect on the protein abundance of either mCherry or GFP in the absence of the *Bach2* 5' UTR (Figures S5C and S5E). These results demonstrate that the 5' UTR of *Bach2* impedes cap-dependent protein translation and is sensitive to eIF4A activity. Therefore, BCR stimulation up-regulates Bach2 protein abundance by activating the mTORC1/eIF4A axis-dependent translation.

BCR engagement and T cell help are transient, and mTORC1 activation and active Bach2 protein translation are supposed to limit to specific B cell subsets at the pre-GC stage. To test this notion, we firstly analyzed the mTORC1 activity in various B cell subsets. mTORC1 stimulates the phosphorylation of ribosomal protein S6 (phospho-S6) at several serine sites via p70S6K. S6 phosphorylation, which can be used to monitor the kinetics of mTORC1 activity in GC responses (Ersching et al., 2017). S6 phosphorylation was obviously up-regulated in both NP-binding activated and memory B cells on day 2 after immunization, although the latter increased less (Figure 6D). On day 5 memory B cells and active precursors reduced phospho-S6 expression to levels similar to those of naïve B cells (Figure 6D). S6 phosphorylation was continually and highly expressed in plasmablasts and PCs, but barely detected in GC B cells on day 5 (Figure 6D).

To examine the kinetics of Bach2 protein expression in vivo, we constructed a Bach2 protein reporter mouse strain (Figures S6A and S6B). Although naïve B cells contained high amounts of *Bach2* mRNA, they expressed very low levels of Bach2 protein due to the lack of mTORC1 activation (Figure 6E). The Bach2 protein reporter was obviously up-regulated in both NP-binding activated and memory B cells on day 2 after immunization, although the latter increased less (Figure 6E). Of note, some plasmablasts displayed an increase of Bach2 protein possibly because they still expressed substantial levels of *Bach2* transcripts (Figure 5A). On day 5 expression of the Bach2 protein reporter in memory B cells and memory precursors returned to the similar levels as those in naïve B cells (Figure 6E). Therefore, these results indicate the similar dynamics of the mTORC1 activity and Bach2 protein abundance in these cells, suggesting a critical role of mTORC1 activity in regulating Bach2 protein abundance. Unexpectedly, GC B cells and their precursors expressed high levels of Bach2 protein reporter (Figure 6E), although the mTORC1 activity is largely silenced in these cells, suggesting that the translation of Bach2 protein is independent of the mTORC1 activity in GC B cells.

Sustained and higher concentrations of Bach2 protein facilitates the generation of memory B cells while antagonizing the GC fate

Transient up-regulation of Bach2 protein in activated B cell favors memory and GC B cell fates (Figure 1). We next asked whether sustained Bach2 protein expression in B cells can disrupt their differentiation programs. To do so, congenically marked CD45.1/2 and CD45.2 wild-type B1-8^{hi} cells were infected with retrovirus expressing GFP and Bach2-IRES-GFP, respectively. Transfected cells were mixed and adoptively transferred into wild-type hosts (CD45.1), followed by NP-OVA immunization 24 h post-transfer (Figure 7A). Enforced Bach2 protein expression did not influence the expansion of either non-NP-binding or NP-binding B cells 3 days after immunization (Figure 7B). However, Bach2-overexpressing NP-binding B cells had an increased propensity to differentiate toward memory B cells at the expense of PC and GC B cells (Figure 7C). Transient IRF4 expression is sufficient to induce the GC program (Ochiai et al., 2013). We observed that Bach2-overexpressing NP-binding B cells significantly down-regulated IRF4 protein expression on day 3 (Figure 7D). Thus, sustained and higher concentrations of Bach2 protein terminate the PC and GC programs while promoting the generation of memory B cells, probably by suppressing IRF4 expression.

Bach2 concentrations control the cell-fate of memory B cell upon recall

Our above results demonstrate that memory B cells down-regulate *Bach2* transcripts and barely express Bach2 protein due to lack of mTORC1 activation. We next sought to explore the roles of Bach2 in the maintenance and recall of memory B cells. Induced *Bach2* ablation did not significantly disrupt the total memory pool or in two functionally distinct memory subpopulations based on the expression of PD-L2 and CD80 (Zuccarino-Catania et al., 2014) (Figure 7E), indicating that Bach2 is dispensable for the maintenance of memory B cells. We next conducted secondary adoptive transfer experiments to investigate whether Bach2 expression in GC-independent memory B cells influences their cell-fate outcomes upon memory recall (Figure S7A). Donor *Bach2*-suffcient memory B cells formed equal numbers of PCs and GC B cells upon memory recall, and had greatly reduced capacity for memory re-entry (Figure 7F). Reporter assay showed that activation-induced cytidine deaminase (*Aicda*)-driven Cre can ablate gene in over 75% of memory B cells (Figure S7B), indicating *Aicda*-Cre can used to delete gene in memory B cells. Donor *Bach2*-defcient memory B cells generated higher frequencies of PCs and lower frequencies of GC B cells (Figure 7F). Moreover, they almost abolished the ability to return to the memory pool (Figure 7F). Interestingly, Bach2 overexpression facilitated memory B cells to differentiate towards GC B cells at the expense of near abolishment of PC differentiation (Figure 7G). Moreover, Bach2 overexpression forced memory B cells to enter the memory pool (Figure 7G), a characteristic of activated B cells. Therefore, Bach2 expression level influences the cell-fate of memory B cells upon antigen recall.

Discussion

BCR affinity-related signals establish a sophisticated transcriptional network governing the expansion of activated B cells and subsequent differentiation into diversified effector cells at the pre-GC stage. The key components of this transcriptional network controlling the PC

and GC B cell fates have been partially identified (Cook et al., 2020; Dhenni and Phan, 2020; Sciammas et al., 2011; Suan et al., 2017b; Willis and Nutt, 2019). In this study we demonstrate that BCR affinity-related signals control Bach2 protein expression kinetics in activated B cells to precisely shape their cell-fate outcomes (Figure S7C). Bach2 serves as a key "fate-determining" transcription factor for memory and GC B cell fates at the pre-GC stage. Concomitantly, BCR affinity-related signals suppress *Bach2* transcription in activated B cells and GC-independent memory B cells, predisposing their cell-fate outcomes during memory recall (Figure S7C). Our study demonstrates that how affinity-related signals control Bach2 expression kinetics in a manner which links to B cell-fate diversification in primary and second immune responses.

Bach2 mRNA contains a complex 5' UTR, and its effective translation requires mTORC1 activation and eIF4A activity. BCR and CD40 signals transiently activate the mTORC1 and consequently promote the translation of Bach2 protein in activated B cells (Figure S7C). Higher-affinity activated B cells are predisposed to receive stronger BCR and CD40 signals when the availability of antigen and subsequent T cell help are limited (Schwickert et al., 2011), and are expected to generate more mTORC1 activity and Bach2 protein. This is evidenced that plasmablasts expressed the highest levels of active mTORC1 and Bach2 protein abundance, and memory B cells expressed the lowest amounts of them among all response B cells. Memory B cells and active precursors gradually reduce Bach2 protein expression when further differentiation due to diminished mTORC1 activation.

BCR and CD40 signaling coordinately drive the expansion of activated B cells and generate lineage-committed transcriptional program by inducing the expression and activity of a series of transcription factors, including Myc, IRF4, and Blimp1 (Calado et al., 2012; Dominguez-Sola et al., 2012; Luo et al., 2018; Ochiai et al., 2013; Sciammas et al., 2006). The *Irf4-Prdm1* loop promotes the expansion of activated B cells and PC differentiation, and our study suggests that this loop can be directly repressed by Bach2. Moreover, in activated B cells IRF4 binds to the AP-1-IRF composite element (AICE) that also embeds canonical AP-1 motif (Ochiai et al., 2013). Bach2 also binds to AP-1 or AICE motif in activated B cells (Hipp et al., 2017) . Therefore, although Bach2 and IRF4 protein are concomitantly up-regulated in activated B cells, they are antagonistic transcription factors and play central but opposing roles for cell-fate decisions. Thus, transient up-regulation of Bach2 protein represents an important mechanism which partially counteracts proliferation of activated B cells and delay their terminal differentiation into PCs, providing a time window for initiating memory and GC B cell differentiation. RNA-seq reveals that *Bach2*-deficient activated B cells reduced the transcripts of *IL-4R* and *IL-21R* (date not shown). IL4 and IL21 signaling is critical for activated B cells to express Bcl6 protein and subsequently differentiate into GC B cells (Chevrier et al., 2017). Bach2 might strengthen IL4 and IL21 signaling in activated B cells to facilitate GC B cell fate.

Several studies have reported that either BCR or CD40 signals down-regulate *Bach2* at the transcript levels (Kometani et al., 2013; Muto et al., 2004; Shinnakasu et al., 2016). Our data further demonstrate that activation of BCR and CD40 induces expression of Bach2 and IRF4 protein, which in turn suppress *Bach2* transcription. Plasmablasts rapidly reduced *Bach2* mRNA expression prior to activated B cells and memory B cells. Consistent with a

previous report (Muto et al., 2004), mature PCs almost silence *Bach2* mRNA expression, resulting in loss of Bach2 protein although they exhibit high mTORC1 activity. Early GC precursors receive stronger BCR and CD40 signals than memory counterparts, and expressed lower amounts of *Bach2* transcript. However, early GC precursors gradually restored *Bach2* transcript when further maturation. The underlying mechanism may be linked to up-regulation of Bcl6 when differentiation towards GC B cells (Shinnakasu et al., 2016). Our results explain the confusing observation that mature GC B cells express higher levels of *Bach2* mRNA than GC-derived memory B cells (Wang et al., 2017). Restoration of *Bach2* transcription in GC B cells appears to be critical for the GC programs. Memory B cells also gradually reduced, but not lost *Bach2* transcript. Graded concentrations of Bach2 in GC-independent memory B cells controlled their cell-fate choice between PCs and GC B cells upon memory recall. Therefore, stimulatory history down-regulates expression of preexisting *Bach2* mRNA in GC-independent memory B cells, predisposing them to generate optimal numbers of PCs and GC B cells upon memory recall. Therefore, at the pre-GC stage, signaling-induced repression of *Bach2* transcript in memory B cells, but not loss, optimizes Bach2 protein expression and cell-fate choices in second immune responses.

In conclusion, our study identifies translational control of Bach2 as a key mechanism underlying affinity-based B cell fate decisions, and highlights a crucial role of Bach2 protein expression kinetics in controlling memory and GC B cell fates at the pre-GC stage. Affinity-based signals up-regulate Bach2 and IRF4 protein levels to suppress *Bach2* transcription in activated B cells and their descendant memory B cells, predisposing the optimal fate choice upon memory recall. Therefore, affinity-related signals induce differential dynamics of Bach2 protein and mRNA expression at the pre-GC stage via distinct mechanisms, and controls B cell fate specification at separate phases of humoral responses.

Limitations of the Study

The main limitation of this study is the precise regulation of IRF4 by Bach2. Bach2 appears to be dispensable for repression of IRF4 in $IRF4^{low}$ activated B cells. However, Bach2 seems to be critical to suppress the transition of $IRF4^{low}$ activated B cells to $IRF4^{high}$ PC-committed B cells via direct repression of Irf4 transcription. IRF4 and Bimp1 form the reciprocal transcription regulatory loop to drive PC differentiation. It is possible that Bach2 indirectly regulates IRF4 via suppression of Blimp1. It would be of great interest to investigate the effect of Bach2 on IRF4 in the absence of Blimp1.

STAR*METHODS

RESOURCE AVAILABILITY

Lead Contact—Further information and requests for resources and reagents should be directed to and will be fulfilled by the Lead Contact, Chuanxin Huang (huangcx@shsmu.edu.cn).

Materials availability—All unique reagents generated in this study are available from the Lead Contact with a completed Materials Transfer Agreement.

Data and Code Availability

- RNA-seq data in this study have been deposited in the GEO repository (GSE180277 and GSE180460). They are publicly available as of the date of publication.
- This paper does not report original code.
- Any additional information required to reanalyze the data reported in this work paper is available from the Lead contact upon request.

EXPERIMENTAL MODEL AND SUBJECT DETAILS

Mice—All mice were crossed on C57BL/6 background. *Bach2*$^{fl/fl}$ mice have been previously described (Zhang et al., 2019). B6 CD45.1 (B6.SJL-Ptprc^{a} Pepc^{b}/BoyJ), B6 CD45.2 (C57BL/6J), *Irf4*$^{fl/fl}$ (B6.129S1-Irf4^{tm1Rdf}/J) Rosa26^{tdTomato}, Rosa26-CreER (B6.129-Gt(ROSA)26Sor$^{tm1(cre/ERT2)Tyj}$/J). *Aicda*^{cre} (B6.129P2-Aicda$^{tm1(cre)Mnz}$/J), OT-II (B6.CgTg(TcraTcrb)425Cbn/J), MD4 (C57BL/6-Tg(IghelMD4)4Ccg/J) and B1-8^{hi} (B6.129P2-Ptrpc^{a}Igh^{tm1Mnz}/J) mice were from Jackson Laboratory. The generation of Bach2^{EGFP} mRNA and protein reporter mice was described in Figures S4 and S6. All mice were housed in specific pathogen-free (SPF) facilities. All animal experiments were reviewed and approved by the Institutional Animal Care and Use Committee (IACUC) of shanghai Jiao Tong University, School of Medicine. Both female and male mice at 8–12 weeks of age were used in the experiments.

Cell lines—Phoenix-Eco cells (ATCC, CRL-3214) were cultured in Dulbecco's modified Eagle's medium (DMEM) containing 10% fetal bovine serum (FBS), 100 unit/mL penicillin and 100 mg/mL streptomycin. Cells are mycoplasma free.

METHOD DETAILS

Adoptive transfers and immunization—Spleens were homogenized by filtering through a 70 μ m cell strainer and red blood cells were lysed with ACK buffer. Resting B and CD4^{+} T cells were purified by negative magnetic-activated cell sorting (MACS) using the mouse B cell isolation Kit and mouse CD4^{+} T cell isolation kit, respectively. To study the early TD response, −5 × 10^{6} B1-8^{hi} B cells (~5 × 10^{5} Igλ NP-specific B cells) were transferred intravenously into recipient mice, along with 2 × 10^{5} OT- II CD4^{+} T cells. The recipients were immunized intraperitoneally with 100μg NP(16)-OVA plus 15μg LPS precipitated with Imject alum 24h post-transfer.

To trace the cell-fates of active precursors, NP-specific IgD^{-}CD19^{+}GF7^{+}CD38^{+} active precursors were FACS-sorted from the animals transferred as described above and immunized with NP-OVA for 3 days. Equal numbers of allotypically marked *Bach2*-sufficient and deficient active precursor B cells (6×10^{3} in total) were transferred into the recipients which received 2 × 10^{5} OT- II CD4^{+} T cells, and were immunized with NP-OVA at the same day as the donor animals. The recipients were sacrificed for analysis on day 4 after transfer of active precursor cells.

For memory B cell maintenance, the adoptive transfer experiments were performed as described above. Six weeks later, deletion of loxP-flanked *Bach2* alleles was induced by oral administration (p.o.) of 2 mg tamoxifen daily for 3 consecutive days. 7 days post-administration, mice were scarified for analysis of memory B cells.

For memory recall, $IgD^{-}CD19^{+}GF7^{-}CD38^{+}$ NP-specific memory B cells were FACS-sorted from the animals transferred as described above and immunized with NP-OVA for 5 days. Sorted memory B cells were transferred into the recipients which were primed with 50μg OVA precipitated with Imject alum 2-4 weeks ago. 24h later, the recipients were boosted with NP(16)- OVA alone, and sacrificed on day 5 post-immunization.

In vitro B cell culture and stimulation—Purified B cells were plated at a concentration of 1×10^{6} cells per 400 μl in round-bottom 48-well plates in complete RPMI media with stimuli for 1-3 d. B cells were stimulated with 10μg/ml goat anti-mouse IgM F(ab')2, 10μg/ml anti-CD40, 5μg/ml LPS, 0.2 μM CpG, 10μM U0126-EtOH, 2μM MK-2206, 100ng/ml Rapmaycin, 50μM T-5224, 10nM Silvestrol as indicated in Figure legends. In some experiments, anti-IgM and anti-CD40 were used at different concentrations. To monitor B cell division, B cells were labeled using CFSE or CTV (Invitrogen) according to the manufacture's protocol, and then transferred to complete medium for culture.

Flow cytometry analysis—Splenocytes were harvested into single-cell suspension as described above. Cells were first blocked with anti-CD 16/32(BD Bioscience), and stained with LIVE/DEAD™ Fixable Violet Dead Cell Stain Kit according to the manufacturer's instructions. Surface staining was performed in the PBS containing 2% fetal bovine serum with fluorescence-tagged antibodies (KEY RESOURCE TABLE). After surface staining, cells were fixed and permeabilized with Foxp3/transcription factor staining buffer set to detect IRF4, Blimp1, Bc16. All the flow cytometry analysis was performed on a LSRFortessa X-20 (BD), and data were analyzed with FlowJo software (Tree Star).

Construction of plasmids—Expressing construct for mouse Bach2 was generated by inserting cDNA encoding mouse Bach2 into retroviral Migr1-GFP or Migr1-Thy1.1 vector. cDNA encoding mCherry was cloned into the Migr1-GFP vector to generate Migr1-mCherry-GFP (control reporter). To generate the *Bach2* 5'UTR reporter, cDNA encompassing the *Bach2* 5'UTR was synthesized, and cloned into upstream of mCherry of control reporter. The sequence of cloning primers was found in KEY RESOURCE TABLE. Short hairpin RNA targeting *Prdm1* sh(*Prdm1*), *Irf4* (sh*Irf4)* or scramble (scr) was cloned into pSIREN-RetroQ-DsRed (Clontech). The targeting sequences were found in KEY RESOURCE TABLE.

Polysome profiling—B cell lysate was prepared using polysome lysis buffer (20mM Tris-HCl pH 7.4, 150mM NaCl, 5 mM MgCl2, 1mM DTT, 100 μg/ml cycloheximide, 1% Triton X-100, 25 U/ml DNase I , 20 U/ml RNase inhibition). Cell lysate was cleared by centrifugation at 20,000×g at 4 °C for 10 min. Clarified lysate was loaded onto a 5–50% linear sucrose gradient (sucrose in 20mM Tris-HCl pH 7.4, 150mM NaCl, 5 mM MgCl2, 1mM DTT, 100 μg/ml cycloheximide, 20 U/ml RNase inhibition) and centrifuged for 2 h in a SW60Ti rotor (Beckman) at 36000 rpm at 4°C. During fractionation using a Gradient

fractionator (Biocomp) the UV profile (260 nm) was measured. Obtained fractions were further purified using RNA Clean & Concentrator™-5 (Zymo Research) and then reverse-transcribed for qPCR analysis.

Retrovirus production and transduction—Virus were prepared by transfecting Phoenix cells (ATCC) with retroviral vectors. Naïve B cells were stimulated with anti-CD180 (0.25 μg/ml) for 24h, then centrifuged at 2000rpm for 1.5 h at 32°C with retroviruses in the presence of polybrene (8μg/ml). and cultured overnight for the second infection as one day before. Transduced cells were then cultured for analysis or transferred immediately into the recipients via tail vein injection.

Computational prediction of RNA structure—The sequence of the 5'UTR of mouse *Bach2* were obtained from the Ensembl Genome Browser. The most abundant transcript was selected for predicting. Prediction of the *Bach2* mRNA 5' UTR was performed using the Mfold program (http://www.unafold.org/).

RNA sequencing and GSEA—A total of ~1×10^4 different B cell subset was sorted using a FACSAria III cell sorter (BD Biosciences) at the core facility of Shanghai Institute of Immunology. cDNA was synthesized and amplified using the SMART-Seq v4 Ultra Low input RNA Kit for Illumina Sequencing. The library for mRNA sequencing was generated using TurePrep DNA Library Prep Kit V2 for Illumnia and sequenced using Illumnia NovaSeq 6000 sequencer. The mapping rate was 96% overall across all the samples in the dataset. HTSeq was used to quantify the gene expression counts from HISAT2 alignment files. Differential expression analysis was performed on the count data using R package DESeq2. P values obtained from multiple tests were adjusted using Benjamini-Hochberg correction. Significantly differentially expressed genes are defined by a Benjamini-Hochberg corrected P value < 0.01 and fold change > 2. Gene set enrichment analysis (GSEA) software was provided by Broad Institute and was used for analysis accordingly to instructions.

Immunoblot analysis—Cells were lysed in 1×SDS lysis buffer and denatured at 95 °C for 10 min. Protein lysates then were resolved in 8–10% Tris-Glycine gels. Samples were incubated with primary antibodies overnight at 4° C. Horseradish peroxidase–conjugated secondary antibodies and ECL reagent (Millipore) were used for detection. Each western blotting was repeated for three times and the representative results were shown.

Real-time PCR—MACS-purified B cells were cultured at 37 °C with varying stimuli and harvested into TRIzol (Invitrogen), then stored at −80° C. RNA was extracted via phenol phase separation and then reverse-transcribed with PrimeScript RT reagent Kit (Takara). Quantitative real-time PCR was carried out with TB Green® Premix Ex Taq™ (Takara). All quantitative data were normalized to the amount of *β-Actin.* Gene specific primers are listed in the supplementary information (KEY RESOURCE TABLE).

QUANTIFICATION AND STATISTICAL ANALYSIS

The number of mice per group, number of replicates and the nature of error bars are indicated in the legend of each figure. Center bars always indicate mean. Statistical significance was determined with Graphpad Prism Version 7.0 using the tests indicated in each figure legend. *P* value < 0.05 is considered statistically significant, and the level of significance was indicated as **P* < 0.05 and ***P* < 0.01. *P*-values >0.05 are considered to be not significant (ns).

Supplementary Material

Refer to Web version on PubMed Central for supplementary material.

Acknowledgments

This work was supported by the National Key R&D Program of China (2021YFA1301403 and 2019YFA0111000), the National Natural Science Foundation of China (31870872, 32070881 and 32000618), Shanghai Science and Technology Committee (20ZR1448800, 20JC1410100) and Innovative research team of high-level local universities in Shanghai (ZDCX20211800).

References

Benhamron S, Hadar R, Iwawaky T, So JS, Lee AH, and Tirosh B (2014). Regulated IRE1-dependent decay participates in curtailing immunoglobulin secretion from plasma cells. European journal of immunology 44, 867–876. [PubMed: 24242955]

Calado DP, Sasaki Y, Godinho SA, Pellerin A, Kochert K, Sleckman BP, de Alboran IM, Janz M, Rodig S, and Rajewsky K (2012). The cell-cycle regulator c-Myc is essential for the formation and maintenance of germinal centers. Nature immunology 13, 1092–1100. [PubMed: 23001146]

Chan TD, Gatto D, Wood K, Camidge T, Basten A, and Brink R (2009). Antigen affinity controls rapid T-dependent antibody production by driving the expansion rather than the differentiation or extrafollicular migration of early plasmablasts. Journal of immunology 183, 3139–3149.

Chevrier S, Kratina T, Emslie D, Tarlinton DM, and Corcoran LM (2017). IL4 and IL21 cooperate to induce the high Bcl6 protein level required for germinal center formation. Immunol Cell Biol 95, 925–932. [PubMed: 28875978]

Cook SL, Franke MC, Sievert EP, and Sciammas R (2020). A Synchronous IRF4-Dependent Gene Regulatory Network in B and Helper T Cells Orchestrating the Antibody Response. Trends in immunology 41, 614–628. [PubMed: 32467029]

Cyster JG, and Allen CDC (2019). B Cell Responses: Cell Interaction Dynamics and Decisions. Cell 177, 524–540. [PubMed: 31002794]

De Silva NS, and Klein U (2015). Dynamics of B cells in germinal centres. Nature reviews. Immunology 15, 137–148.

Dhenni R, and Phan TG (2020). The geography of memory B cell reactivation in vaccine-induced immunity and in autoimmune disease relapses. Immunological reviews 296, 62–86. [PubMed: 32472583]

Dominguez-Sola D, Victora GD, Ying CY, Phan RT, Saito M, Nussenzweig MC, and Dalla-Favera R (2012). The proto-oncogene MYC is required for selection in the germinal center and cyclic reentry. Nature immunology 13, 1083–1091. [PubMed: 23001145]

Elsner RA, and Shlomchik MJ (2020). Germinal Center and Extrafollicular B Cell Responses in Vaccination, Immunity, and Autoimmunity. Immunity 53, 1136–1150. [PubMed: 33326765]

Ersching J, Efeyan A, Mesin L, Jacobsen JT, Pasqual G, Grabiner BC, Dominguez-Sola D, Sabatini DM, and Victora GD (2017). Germinal Center Selection and Affinity Maturation Require Dynamic Regulation of mTORC1 Kinase. Immunity 46, 1045–1058 e1046. [PubMed: 28636954]

Gaudette BT, Jones DD, Bortnick A, Argon Y, and Allman D (2020). mTORC1 coordinates an immediate unfolded protein response-related transcriptome in activated B cells preceding antibody secretion. Nat Commun 11, 723. [PubMed: 32024827]

Gitlin AD, von Boehmer L, Gazumyan A, Shulman Z, Oliveira TY, and Nussenzweig MC (2016). Independent Roles of Switching and Hypermutation in the Development and Persistence of B Lymphocyte Memory. Immunity 44, 769–781. [PubMed: 26944202]

Hipp N, Symington H, Pastoret C, Caron G, Monvoisin C, Tarte K, Fest T, and Delaloy C (2017). IL-2 imprints human naive B cell fate towards plasma cell through ERK/ELK1-mediated BACH2 repression. Nat Commun 8, 1443. [PubMed: 29129929]

Huang C, Geng H, Boss I, Wang L, and Melnick A (2014). Cooperative transcriptional repression by BCL6 and BACH2 in germinal center B-cell differentiation. Blood 123, 1012–1020. [PubMed: 24277074]

Ise W, and Kurosaki T (2019). Plasma cell differentiation during the germinal center reaction. Immunological reviews 288, 64–74. [PubMed: 30874351]

Iwakoshi NN, Lee AH, Vallabhajosyula P, Otipoby KL, Rajewsky K, and Glimcher LH (2003). Plasma cell differentiation and the unfolded protein response intersect at the transcription factor XBP-1. Nature immunology 4, 321–329. [PubMed: 12612580]

Kaji T, Ishige A, Hikida M, Taka J, Hijikata A, Kubo M, Nagashima T, Takahashi Y, Kurosaki T, Okada M, et al. (2012). Distinct cellular pathways select germline-encoded and somatically mutated antibodies into immunological memory. The Journal of experimental medicine 209, 2079–2097. [PubMed: 23027924]

Kometani K, Nakagawa R, Shinnakasu R, Kaji T, Rybouchkin A, Moriyama S, Furukawa K, Koseki H, Takemori T, and Kurosaki T (2013). Repression of the transcription factor Bach2 contributes to predisposition of IgG1 memory B cells toward plasma cell differentiation. Immunity 39, 136–147. [PubMed: 23850379]

Kurosaki T, Kometani K, and Ise W (2015). Memory B cells. Nature reviews. Immunology 15, 149–159.

Luo W, Weisel F, and Shlomchik MJ (2018). B Cell Receptor and CD40 Signaling Are Rewired for Synergistic Induction of the c-Myc Transcription Factor in Germinal Center B Cells. Immunity 48, 313–326 e315. [PubMed: 29396161]

Muto A, Ochiai K, Kimura Y, Itoh-Nakadai A, Calame KL, Ikebe D, Tashiro S, and Igarashi K (2010). Bach2 represses plasma cell gene regulatory network in B cells to promote antibody class switch. The EMBO journal 29, 4048–4061. [PubMed: 20953163]

Muto A, Tashiro S, Nakajima O, Hoshino H, Takahashi S, Sakoda E, Ikebe D, Yamamoto M, and Igarashi K (2004). The transcriptional programme of antibody class switching involves the repressor Bach2. Nature 429, 566–571. [PubMed: 15152264]

Ochiai K, Maienschein-Cline M, Simonetti G, Chen J, Rosenthal R, Brink R, Chong AS, Klein U, Dinner AR, Singh H, and Sciammas R (2013). Transcriptional regulation of germinal center B and plasma cell fates by dynamical control of IRF4. Immunity 38, 918–929. [PubMed: 23684984]

Ochiai K, Muto A, Tanaka H, Takahashi S, and Igarashi K (2008). Regulation of the plasma cell transcription factor Blimp-1 gene by Bach2 and Bcl6. International Immunology 20, 453–460. [PubMed: 18256039]

Ohkubo Y, Arima M, Arguni E, Okada S, Yamashita K, Asari S, Obata S, Sakamoto A, Hatano M, J OW, et al. (2005). A role for c-fos/activator protein 1 in B lymphocyte terminal differentiation. Journal of immunology 174, 7703–7710.

Pape KA, Taylor JJ, Maul RW, Gearhart PJ, and Jenkins MK (2011). Different B cell populations mediate early and late memory during an endogenous immune response. Science 331, 1203–1207. [PubMed: 21310965]

Paus D, Phan TG, Chan TD, Gardam S, Basten A, and Brink R (2006). Antigen recognition strength regulates the choice between extrafollicular plasma cell and germinal center B cell differentiation. The Journal of experimental medicine 203, 1081–1091. [PubMed: 16606676]

Phan TG, Paus D, Chan TD, Turner ML, Nutt SL, Basten A, and Brink R (2006). High affinity germinal center B cells are actively selected into the plasma cell compartment. The Journal of experimental medicine 203, 2419–2424. [PubMed: 17030950]

Reth M, and Wienands J (1997). Initiation and processing of signals from the B cell antigen receptor. Annual review of immunology 15, 453–479.

Schwickert TA, Victora GD, Fooksman DR, Kamphorst AO, Mugnier MR, Gitlin AD, Dustin ML, and Nussenzweig MC (2011). A dynamic T cell-limited checkpoint regulates affinity-dependent B cell entry into the germinal center. The Journal of experimental medicine 208, 1243–1252. [PubMed: 21576382]

Sciammas R, Li Y, Warmflash A, Song Y, Dinner AR, and Singh H (2011). An incoherent regulatory network architecture that orchestrates B cell diversification in response to antigen signaling. Molecular systems biology 7, 495. [PubMed: 21613984]

Sciammas R, Shaffer AL, Schatz JH, Zhao H, Staudt LM, and Singh H (2006). Graded expression of interferon regulatory factor-4 coordinates isotype switching with plasma cell differentiation. Immunity 25, 225–236. [PubMed: 16919487]

Shapiro-Shelef M, and Calame K (2005). Regulation of plasma-cell development. Nat Rev Immunol 5, 230–242. [PubMed: 15738953]

Shih TA, Meffre E, Roederer M, and Nussenzweig MC (2002). Role of BCR affinity in T cell dependent antibody responses in vivo. Nature immunology 3, 570–575. [PubMed: 12021782]

Shinnakasu R, Inoue T, Kometani K, Moriyama S, Adachi Y, Nakayama M, Takahashi Y, Fukuyama H, Okada T, and Kurosaki T (2016). Regulated selection of germinal-center cells into the memory B cell compartment. Nature immunology 17, 861–869. [PubMed: 27158841]

Suan D, Krautler NJ, Maag JLV, Butt D, Bourne K, Hermes JR, Avery DT, Young C, Statham A, Elliott M, et al. (2017a). CCR6 Defines Memory B Cell Precursors in Mouse and Human Germinal Centers, Revealing Light-Zone Location and Predominant Low Antigen Affinity. Immunity 47, 1142–1153 e1144. [PubMed: 29262350]

Suan D, Sundling C, and Brink R (2017b). Plasma cell and memory B cell differentiation from the germinal center. Current opinion in immunology 45, 97–102. [PubMed: 28319733]

Taylor JJ, Pape KA, and Jenkins MK (2012). A germinal center-independent pathway generates unswitched memory B cells early in the primary response. The Journal of experimental medicine 209, 597–606. [PubMed: 22370719]

Taylor JJ, Pape KA, Steach HR, and Jenkins MK (2015). Humoral immunity. Apoptosis and antigen affinity limit effector cell differentiation of a single naive B cell. Science 347, 784–787. [PubMed: 25636798]

Tellier J, Shi W, Minnich M, Liao Y, Crawford S, Smyth GK, Kallies A, Busslinger M, and Nutt SL (2016). Blimp-1 controls plasma cell function through the regulation of immunoglobulin secretion and the unfolded protein response. Nature immunology 17, 323–330. [PubMed: 26779600]

Turner JS, Benet ZL, and Grigorova IL (2020). Signals 1, 2 and B cell fate or: Where, when and for how long? Immunological reviews 296, 9–23. [PubMed: 32470215]

Venturutti L, Teater M, Zhai A, Chadburn A, Babiker L, Kim D, Beguelin W, Lee TC, Kim Y, Chin CR, et al. (2020). TBL1XR1 Mutations Drive Extranodal Lymphoma by Inducing a Pro-tumorigenic Memory Fate. Cell 182, 297–316 e227. [PubMed: 32619424]

Victora GD, and Nussenzweig MC (2012). Germinal centers. Annual review of immunology 30, 429–457.

Wang Y, Shi J, Yan J, Xiao Z, Hou X, Lu P, Hou S, Mao T, Liu W, Ma Y, et al. (2017). Germinal-center development of memory B cells driven by IL-9 from follicular helper T cells. Nature immunology 18, 921–930. [PubMed: 28650481]

Willis SN, and Nutt SL (2019). New players in the gene regulatory network controlling late B cell differentiation. Current opinion in immunology 58, 68–74. [PubMed: 31132512]

Wolfe AL, Singh K, Zhong Y, Drewe P, Rajasekhar VK, Sanghvi VR, Mavrakis KJ, Jiang M, Roderick JE, Van der Meulen J, et al. (2014). RNA G-quadruplexes cause eIF4A-dependent oncogene translation in cancer. Nature 513, 65–70. [PubMed: 25079319]

Zhang H, Hu Q, Zhang M, Yang F, Peng C, Zhang Z, and Huang C (2019). Bach2 Deficiency Leads to Spontaneous Expansion of IL-4-Producing T Follicular Helper Cells and Autoimmunity. Front Immunol 10, 2050. [PubMed: 31552021]

Zuccarino-Catania GV, Sadanand S, Weisel FJ, Tomayko MM, Meng H, Kleinstein SH, Good-Jacobson KL, and Shlomchik MJ (2014). CD80 and PD-L2 define functionally distinct memory B

cell subsets that are independent of antibody isotype. Nature immunology 15, 631–637. [PubMed: 24880458]

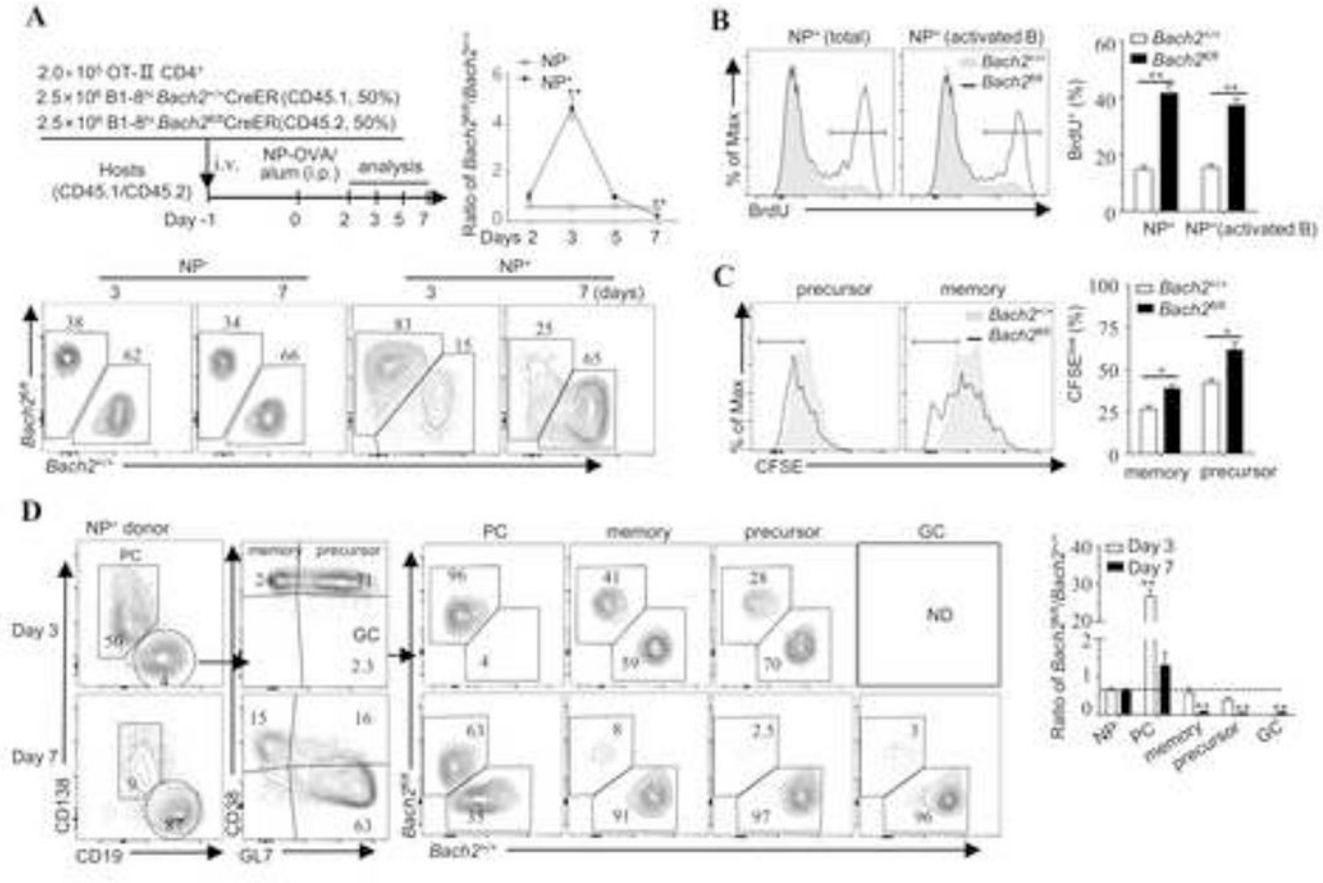

Figure 1. Bach2 restrains activated B cell expansion and PC differentiation.

(A) Diagrammatic representation of the experimental protocol. Flow cytometric analysis of the ratio of *Bach2*$^{fl/fl}$ relative to *Bach2*$^{+/+}$ compartments in donor NP^{-} and NP^{+} cells at indicated days and quantifications. (B) Flow cytometric analysis and quantifications of percent BrdU^{+} cells in donor NP-specific cells and activated B cells on day 2. (C) Flow cytometric analysis of CFSE dilution in active precursors and memory B cells on day 3 and quantifications. (D) Flow cytometric analysis of the ratio of *Bach2*$^{fl/fl}$ relative to *Bach2*$^{+/+}$ compartments in indicated donor NP-specific effector subsets and quantifications. Data are means ± SEM and are representative of at least two independent experiments. ND, undetected. **P* <0.05 and ***P* <0.01 (two-tailed t-test). See also Figures S1 and S2.

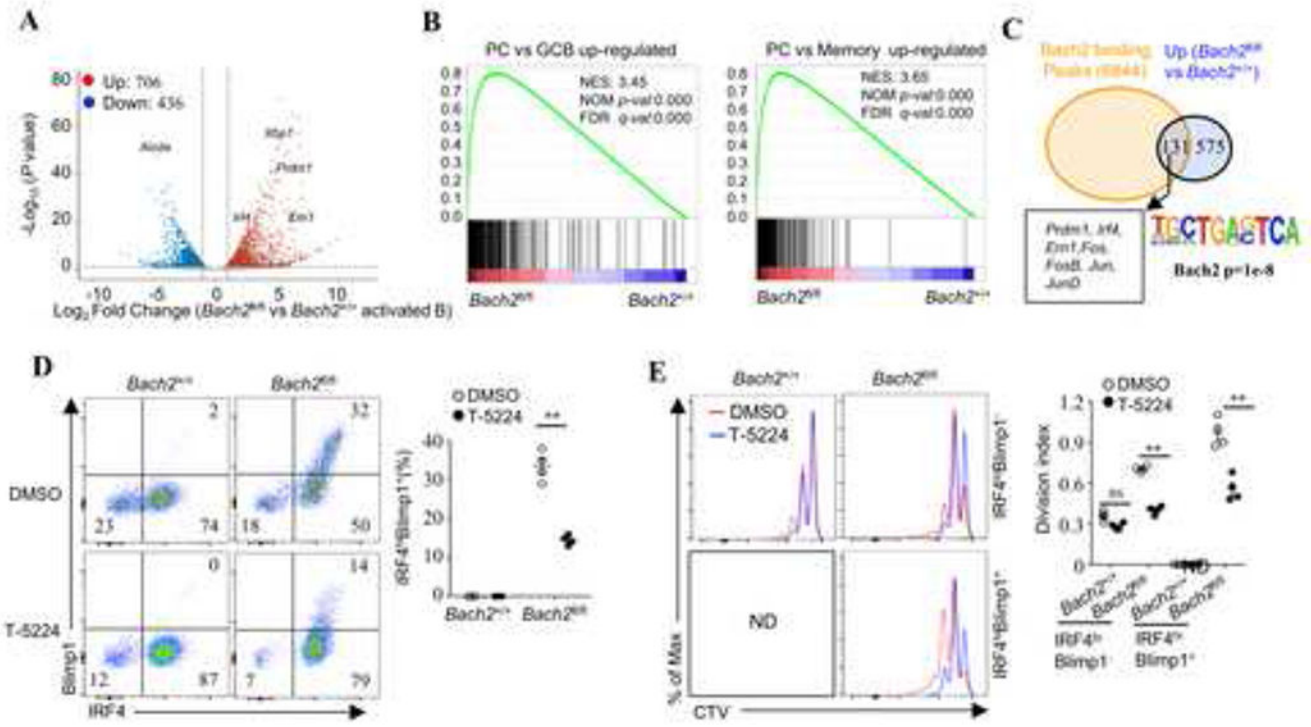

Figure 2. Bach2 directly represses the *Irf4-Prdm1* axis in activated B cells.

(A) Volcano plots showing differential expression genes in *Bach2*$^{fl/fl}$ versus *Bach2*$^{+/+}$ activated B cells. (B) GSEA of up-regulated genes in PCs relative to their expression in GC B cells or memory B cells. (C) The diagram showing Bach2 direct target genes which were up-regulated in *Bach2*-deficient activated B cells and contained at least one Bach2 binding site within 5 kb of TSS. Bottom panel displays overrepresented top sequence motif enriched at these Bach2-bound regions. (D) Flow cytometric analysis and quantifications of percent IRF4^{hi}Blimp1^{+} subset in B cells stimulated with 2.5 μg/ml α-IgM antibody for 72 h in the presence of the c-Fos inhibitor T-5224 (50 μM). (E) CTV dilution in IRF4^{hi}Blimp1^{+} and IRF4^{lo} Blimp1$^{−}$ activated B cells as described in D. The graph depicts the division index of each genotype. Data are means ± SEM (D, E) and are representative of at least two independent experiments, ns, not significance and ** P <0.01 (two-tailed t-test). See also Figure S3.

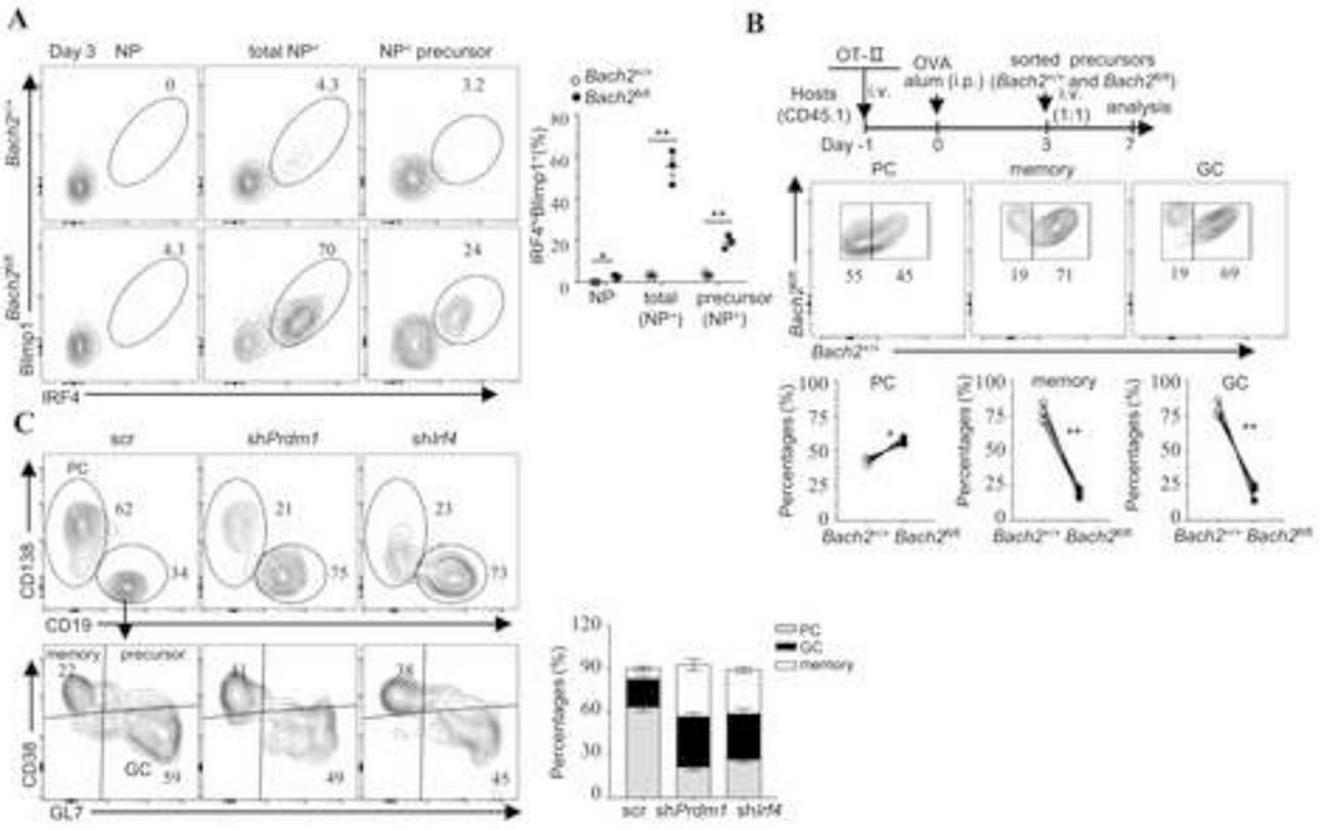

Figure 3. Bach2 represses the *Irf4-Prdm1* axis to enforce memory and GC B cell fates.

The adoptive transfer experiment and immunization was described above (Figure 1A). (A) Flow cytometric analysis and quantifications of percent $IRF4^{hi}Blimp1^{+}$ cells in indicated donor NP-specific populations on day 3 after immunization. (B) Donor *Bach2*$^{+/+}$ (CD45.2/CD45.1) and *Bach2*$^{fl/fl}$ (CD45.2) NP-specific active precursors were isolated 3 days post-immunization and mixed at a ratio of 1:1, and adoptively transferred into wild-type mice ($CD45.1^{+}$) immunized at the same time as the donor animals. Flow cytometric analysis and quantifications of the percentages of each compartment among indicated donor effector subsets. (C) *Bach2*-deficient B1-8^{hi} cells were infected with retrovirus virus expressing scr (scramble), sh*Prdm1* or sh*Irf4,* and adoptively transferred into the recipients and immunized as described in Figure 1A. Flow cytometric analysis of and quantifications of indicated effector subsets in donor transfected NP^{+} cells. Data are means ± SEM and are representative of at least two independent experiments. **P* <0.05 and ***P* <0.01 (two-tailed t-test).

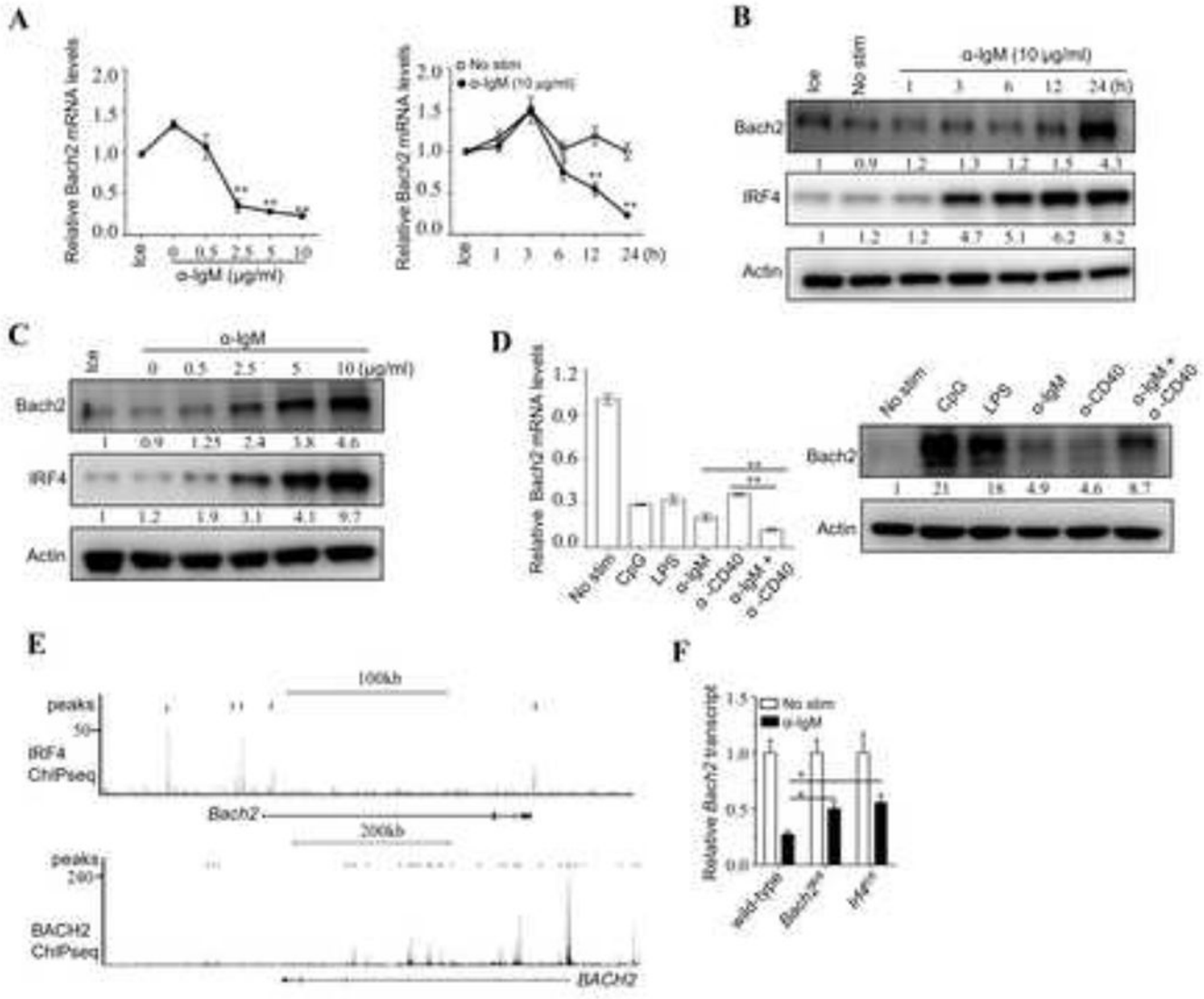

Figure 4. BCR stimulation represses *Bach2* transcription, but increases its protein abundances.

(A) qPCR analysis of *Bach2* mRNA abundance in splenic B cells treated with various concentrations of α-IgM antibody for the indicated times. No stim, no stimulation. (B-C) Immunoblot analysis of indicated protein in splenic B cells as described in **A**. (D) Immunoblotting and qPCR analysis of Bach2 protein and mRNA abundance in splenic B cells stimulated with various stimulators. All qPCR data were normalized within each sample to *β-Actin* and further normalized to the un-stimulated ice sample, which is set to 1 (A, D). (E) The illustration depicting ChIP-seq tracks of BACH2 and IRF4 at the *Bach2* gene in human and mouse activated B cells, respectively, by analyzing published dataset (GSE102460 and GSE46607). (F) qPCR analysis of *Bach2* mRNA abundance in indicated splenic B cells treated with α-IgM antibody (10 μg/ml) for 24 h. Data are means ± SEM (A, D, F) and are representative of at least two independent experiments. **P* <0.05 and ***P* <0.01 (two-tailed t-test).

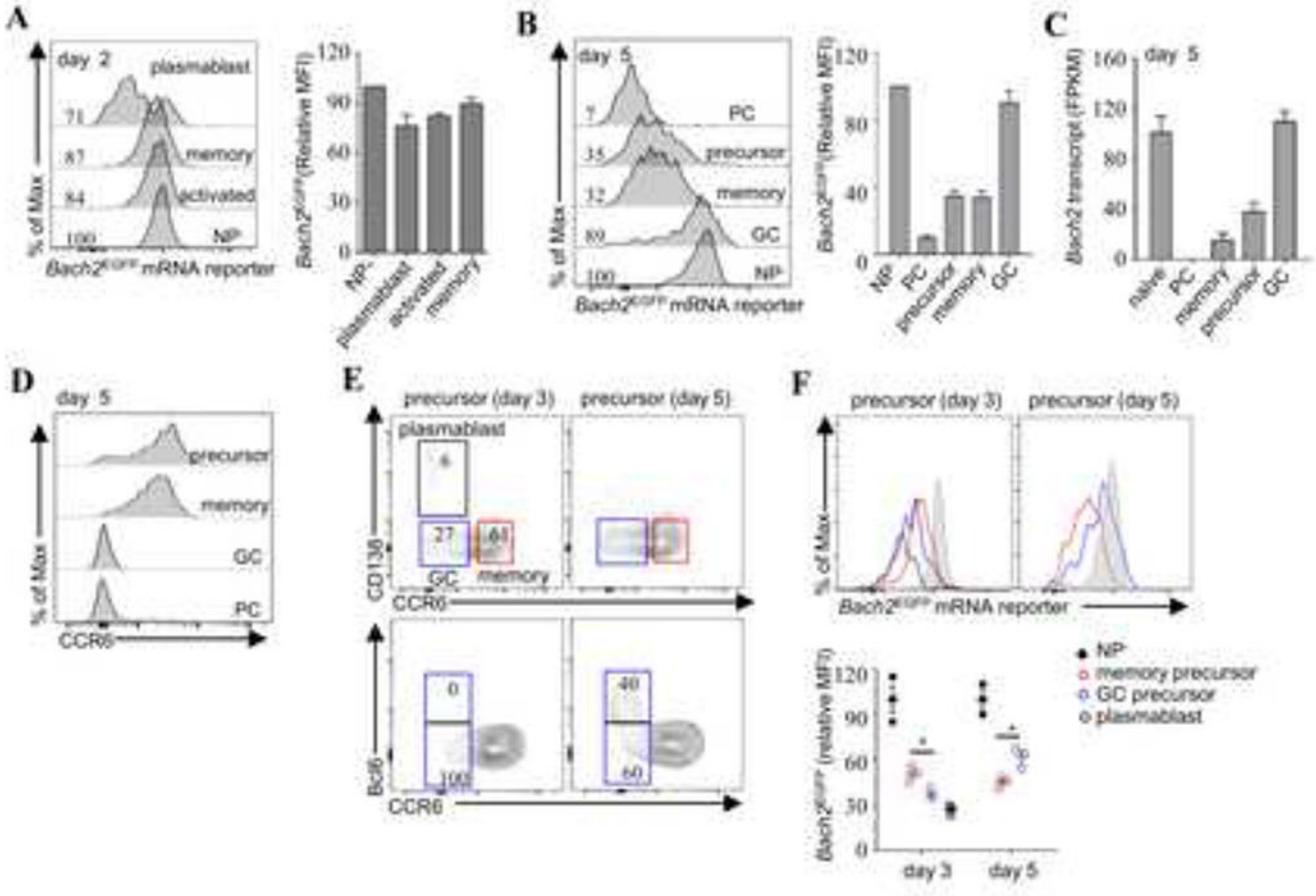

Figure 5. Kinetics of *Bach2* mRNA expression in activated B cells and various effector subsets.

B cells from the B1-8^{hi} *Bach2*^{EGFP} mRNA reporter mice were adoptively transferred into allotypically marked recipients, and then these recipients were immunized with NP-OVA (A-F). (A-B) Flow cytometric analysis of the *Bach2*^{EGFP} mRNA reporter in donor NP^{+} cells at indicated days after immunization and quantifications. (C) FPKM values of *Bach2* in indicated cell populations based on RNA-seq data. (D) Flow cytometric analysis of CCR6 expression in various effector cells on day 5. (E) Identification of CD138^{+}CD19^{+} plasmablasts, CD138^{-}CCR6^{-}CD19^{+} GC precursors, CD138^{-}CCR6^{+}CD19^{+} memory precursors in CD38^{+}GL7^{+}active precursors on day 3 and day 5 after immunization. (F) Flow cytometric plots showing *Bach2* mRNA reporter expression in various precursors and quantifications. The relative MFI of *Bach2* mRNA reporter was calculated after normalization to donor NP^{-} B cells (A-B, F). Data are means ± SEM and are representative of at least two independent experiments. **P* <0.05 and ***P* <0.01 (two-tailed t-test). See also Figure S4.

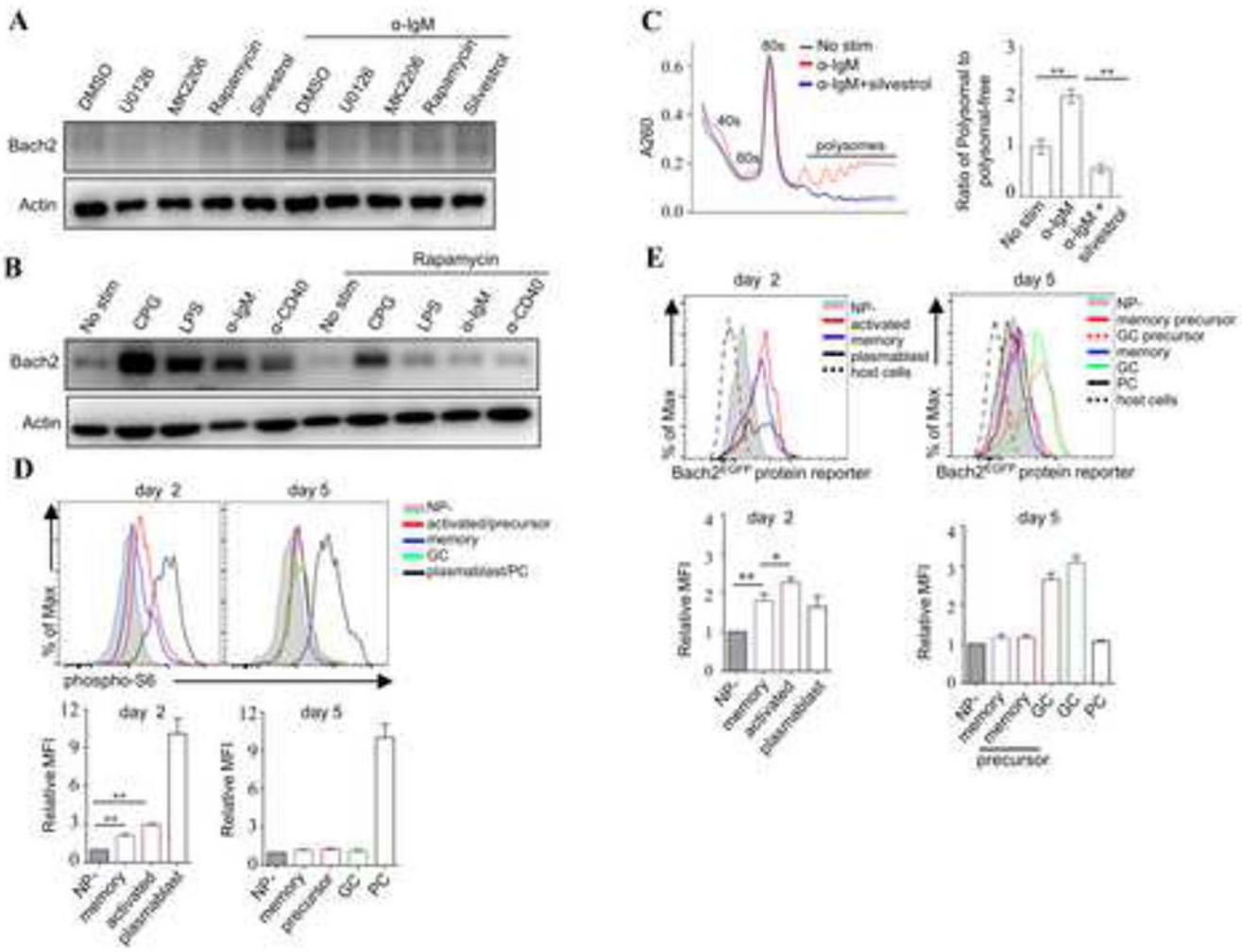

Figure 6. Kinetics of Bach2 protein expression in activated B cells and various effector subsets.

(A) Immunoblot analysis of Bach2 protein in B cells treated with or without indicated inhibitor in the presence of 10 μg/ml α-IgM antibody for 24 h. (B) Immunoblot analysis of Bach2 protein in B cells treated as indicated for 24 h. (C) Polysome profiles of B cells treated as indicated for 12 h. The graph showing the ration of *Bach2* transcript on pooled polysomal fractions relative to that on polysome-free fraction after normalization with *β-Actin.* (D-E) Flow cytometric analysis of phospho-S6 and $Bach2^{EGEP}$ protein reporter in indicated subsets and quantifications. Data are means ± SEM and are representative of at least two independent experiments. $^{**}P<0.01$ (two-tailed t-test). See also Figures S5 and S6.

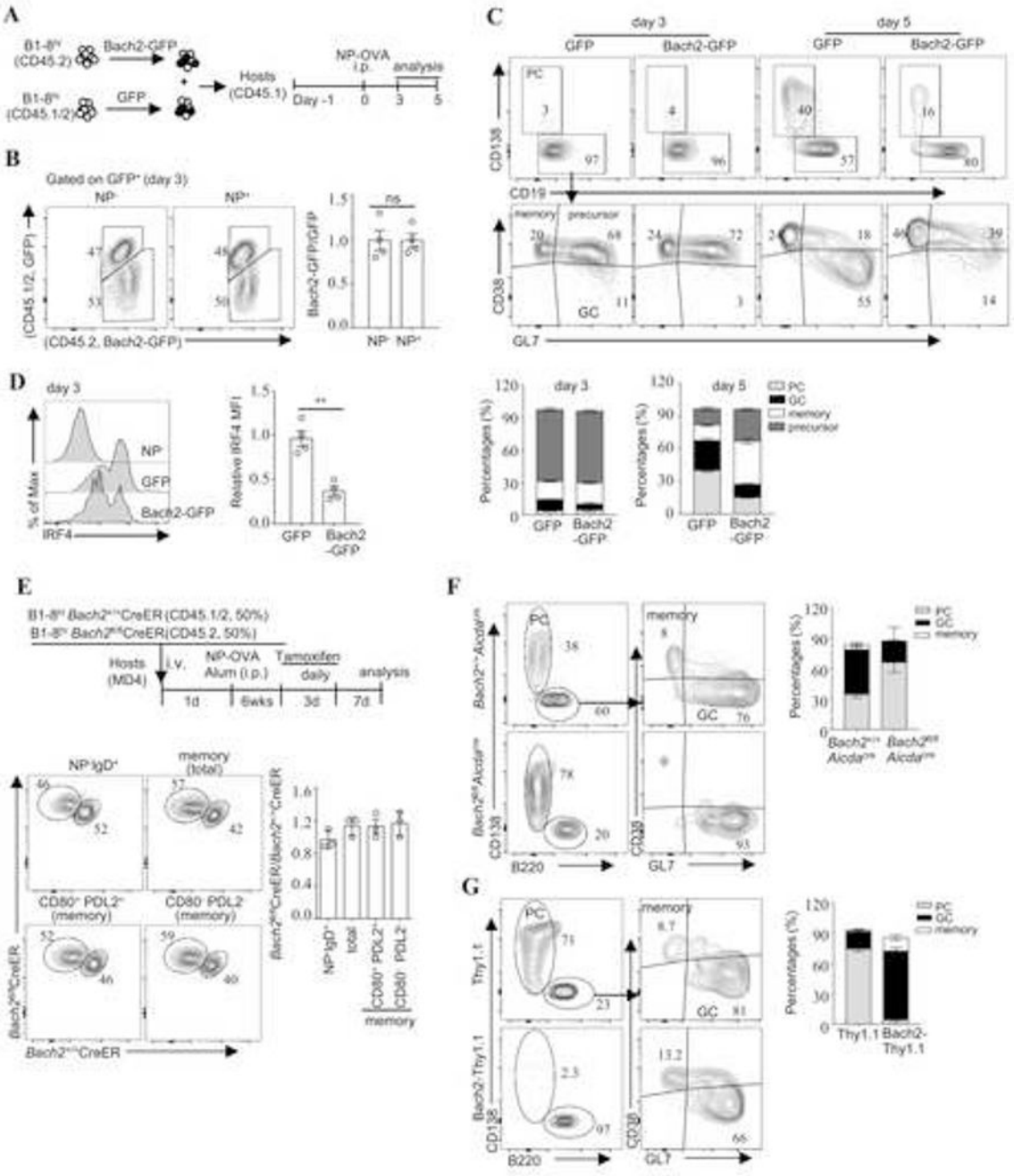

Figure 7. Bach2 concentration regulates memory B cell fate and memory recall.

(A) Diagrammatic representation of the experimental protocol. (B) Flow cytometric analysis and quantifications of the ratio of Bach2-GFP expressing cells relative to GFP expressing cells in donor NP^- and NP^+ B cells at day 3 after immunization. (C) Flow cytometric analysis of percentages of indicated effector subsets in GFP or Bach2-GFP expressing NP^+ donor cells. (D) Flow cytometric analysis and quantifications of IRF4 expression in GFP or Bach2-GFP expressing donor NP^+ cells on day 3. (E) Diagrammatic representation of the experimental protocol. Flow cytometric analysis and quantifications of the ratio of *Bach2*$^{fl/fl}$

relative to *Bach2*$^{+/+}$ compartment in each memory B cell subset. (F-G) Flow cytometric analysis and quantifications of the percentages of each compartment among indicated donor effector subsets on day 5 after antigen recall. Each circle represents one mouse. Data are means ± SEM and are representative of at least two independent experiments. * $P < 0.05$ and ** $P < 0.01$ (two-tailed t-test). See also Figure S7.

KEY RESOURCES TABLE

REAGENT or RESOURCE	SOURCE	IDENTIFIER
Antibodies		
anti- CD45R/B220	BD Biosciences	Cat# 553092, RRID:AB_398531
anti- CD45R/B220	BD Biosciences	Cat# 553087, RRID:AB_394618
anti- CD45R/B220	BD Biosciences	Cat# 561878, RRID:AB_394619
anti- CD45R/B220	BD Biosciences	Cat# 561881, RRID:AB_394458
anti- CD45R/B220	BioLegend	Cat# 103241, RRID:AB_11204069
anti- CD19	BioLegend	Cat# 115543, RRID:AB_11218994
anti- IgD- Biotin	Thermo Fisher Scientific	Cat# 13-5993-82, RRID:AB_466860
anti- IgD	Thermo Fisher Scientific	Cat# 48-5993-82, RRID:AB_1272202
anti- IgD	BioLegend	Cat# 405715, RRID:AB_10660304
anti- CD138 (Syndecan-1)	BioLegend	Cat# 142514, RRID:AB 2562198
anti- CD138	BD Biosciences	Cat# 561070, RRID: AB_395000
anti- CD79b (Igβ)	BioLegend	Cat# 132808, RRID:AB_2632916
anti- CD38	Thermo Fisher Scientific	Cat# 17-0381-81, RRID:AB_469381
anti- CD38	BioLegend	Cat# 102722, RRID:AB_2563333
anti- CD38	BioLegend	Cat# 102718, RRID:AB_2275531
anti- GL7 (T and B cell Activation Marker)	BioLegend	Cat# 144614, RRID: AB_2563292
anti- GL7 (T and B cell Activation Marker)	BioLegend	Cat# 144606, RRID:AB_2562185
anti- GL7 (T and B cell Activation Marker)	BioLegend	Cat# 144603, RRID:AB_2561696
anti- CD80 (B7-1)	Thermo Fisher Scientific	Cat# 17-0801-81, RRID:AB_469416
anti- CD273 (B7-DC, PD-L2)	BioLegend	Cat# 107217, RRID:AB_2728125
anti- CD196 (CCR6)	BioLegend	Cat# 129813, RRID:AB 1877148
anti- CD45.1	Thermo Fisher Scientific	Cat# 11-0453-81, RRID:AB 465057
anti- CD45.1	Thermo Fisher Scientific	Cat# 45-0453-82, RRID: AB_1107003
anti- CD45.1	BioLegend	Cat# 110737, RRID:AB_11204076
anti- CD45.2	Thermo Fisher Scientific	Cat# 56-0454-81, RRID:AB 657753
anti- CD45.2	Thermo Fisher Scientific	Cat# 45-0454-82, RRID:AB_953590
anti- CD45.2	BioLegend	Cat# 109841, RRID:AB_2563485
anti- CD45.2	Thermo Fisher Scientific	Cat# 11-0454-81, RRID:AB_465060
anti- CD4	BioLegend	Cat# 100449, RRID:AB_2564587
anti- CD4	Thermo Fisher Scientific	Cat# 17-0041-82, RRID:AB_469320
anti- IRF4	BioLegend	Cat# 646406, RRID:AB_2563267
anti- IRF4	BioLegend	Cat# 646404, RRID:AB_2563005
anti- IRF4	BioLegend	Cat# 646414, RRID:AB_2728480
anti- BrdU	BioLegend	Cat# 339808, RRID:AB_10895898
anti- Bcl6	BD Biosciences	Cat# 563363, RRID:AB_2738159
anti- Blimp1/Prdm1	BD Biosciences	Cat# 563643, RRID:AB 2738342

REAGENT or RESOURCE	SOURCE	IDENTIFIER
Phospho-Akt (Ser473) (D9E) Rabbit mAb	Cell Signaling Technologies	Cat# 4060S, RRID:AB_2315049
Phospho-S6 Ribosomal Protein (Ser235/236) (D57.2.2E) Rabbit mAb	Cell Signaling Technologies	Cat# 4858T, RRID:AB_916156
Goat anti-Rabbit IgG (H+L) Highly Cross-Adsorbed Secondary Antibody	Thermo Fisher Scientific	Cat# A32733, RRID:AB_2633282
Goat anti-Rabbit IgG (H+L) Highly Cross-Adsorbed Secondary Antibody	Thermo Fisher Scientific	Cat# A11034, RRID:AB_2576217
anti-β-Actin	Sigma-Aldrich	Cat# A5441, RRID:AB_476744
IRF-4 (D9P5H) Rabbit mAb	Cell Signaling Technologies	Cat# 15106S, RRID:AB_2798709
HRP-labeled Goat Anti-Mouse IgG (H+L) antibody	Beyotime	Cat# A0216, RRID:AB_2860575
HRP-labeled Goat Anti-Rabbit IgG (H+L) antibody	Beyotime	Cat# A0208, RRID:AB_2892644
anti-Bach2 polyclonal antibody	Huang et al. (2014)	N/A
Chemicals, Peptides, and Recombinant Proteins		
AF647 sreptavidin	BioLegend	Cat# 405237
PE-CY7 sreptavidin	BioLegend	Cat# 405206
Fixable Viability Stain 700	BD Biosciences	Cat# 564997
Fixable Viability Stain 780	BD Biosciences	Cat# 565388
Imject™ Alum Adjuvant	Thermo Fisher Scientific	Cat# 77161
NIP(16)-BSA-Biotin	Biosearch Technologies	Cat# N-1027
NP(29)-PE	Biosearch Technologies	Cat# N-5070
NP(16)-OVAL(Ovalbumin)	Biosearch Technologies	Cat# N-5051
Ovalbumin(Oval)	Biosearch Technologies	Cat# O-1000
LPS(055:B5)	Sigma	Cat# L2880
Tamoxifen	Sigma	Cat# T5648
Polybrene Transfection Reagent	Millipore	Cat# TR-1003-G
BRDU	Sigma	Cat# B5002
Anti-CD180	BD Biosciences	Cat# 562191
Anti-CD40	eBioscience	Cat# 16-0402-38
Affinipure F(ab')$_2$ Fragment Goat anti-mouse IgM	Jackson ImmunoResearch	Cat# 115-006-020
CPG	InvivoGen	Cat# tlrl-1826
U0126-EtOH	selleck	Cat# S1102
MK-2206 2HCL	selleck	Cat# S1078
Silvestrol	Biovision	Cat# B2417
DTT	VWR	Cat# 0281
DNase I	Qiagen	Cat# 79256
Murine RNase Inhibitor	Vazyme	Cat# DD4102
cycloheximide	selleck	Cat# S7418
Rapamycin	selleck	Cat# S1039
T-5224	selleck	Cat# S8966
Critical Commercial Assays		
CaspGLow™ Fluorescein Active Caspase-3 Staining Kit	Biovision	Cat# K183

REAGENT or RESOURCE	SOURCE	IDENTIFIER
eBioscience™ Foxp3 / Transcription Factor Staining Buffer Set	ThermoFisher Scientific	Cat# 00-5523-00
Phosflow™ Fix Buffer I	BD Bioscience	Cat# 557870
Immobilon Western Chemiluminescent HRP Substrate	Millipore	Cat# WBKLS0500
EasySep™ Mouse $CD4^+$ T Cell Isolation Kit	STEMCELL Technologies	Cat#19852
B Cell Isolation Kit	Miltenyi Biotec	Cat# 130-090-862
CellTrace CFSE Cell Proliferation Kit	Thermo Fisher Scientific	Cat# C34554
APC-Brdu kit	BD Biosciences	Cat# 552598
RNA Clean & Concentrato-5	Zymo Research	Cat# R1015
Deposited Data		
Raw data files for RNA-seq of B subsets	This paper	GSE180460
Raw data files for RNA-seq of activated B	This paper	GSE180277
Datasets for BACH2 Chip-seq	Hipp et al. (2017)	GSE102460
Datasets for IRF4 Chip-seq	Ochiai et al. (2013)	GSE46607
Experimental Models: Cell Lines		
Phoenix-Eco cell line	ATCC	Cat# CRL-3214, RRID:CVCL_H717
Experimental Models: Organisms/Strains		
Mouse: B6 CD45.2: C57BL/6J	The Jackson Laboratory	RRID:IMSR_JAX:000664
Mouse: B6 CD45.1: B6.SJL-$Ptprc^a$ $Pepc^b$/BoyJ	The Jackson Laboratory	RRID:IMSR_JAX:002014
Mouse: $Aicda^{Cre}$: B6.129P2-$Aicda^{tm1(cre)Mnz}$/J	The Jackson Laboratory	RRID:IMSR_JAX:007770
Mouse: Rosa26-CreER: B6.129-Gt(ROSA)26$Sor^{tm1(cre/ERT2)Tyj}$/J	The Jackson Laboratory	RRID:IMSR_JAX:008463
Mouse: B1-8hi: B6.129P2-$Ptrpc^a$$Igh^{tm1Mnz}$/J	The Jackson Laboratory	RRID:IMSR_JAX:007594
Mouse: MD4: C57BL/6-Tg(IghelMD4)4Ccg/J	The Jackson Laboratory	RRID:IMSR_JAX:002595
Mouse: $Rosa26^{Tdtomato}$: B6.Cg-Gt(ROSA)26$Sor^{tm14(CAG-tdTomato)Hze}$/J	The Jackson Laboratory	RRID:IMSR_JAX:007914
Mouse: OT-II : B6.CgTg(TcraTcrb)425Cbn/J	The Jackson Laboratory	RRID:IMSR_JAX:4194
Mouse: Irf4fl/fl: B6.129S1-$Irf4^{tm1Rdf}$/J	The Jackson Laboratory	RRID:IMSR_JAX:009380
Mouse: $Bach2^{fl/fl}$	Zhang et al (2019)	N/A
Mouse: $Bach2^{EGFP}$ RNA reporter mice	This paper	N/A
Mouse: $Bach2^{EGFP}$ protein reporter mice	This paper	N/A
Oligonucleotides		
Primers for RT-qPCR, see Table S1	This paper	N/A
Primers for CHIP-qPCR, see Table S1	This paper	N/A
Primers for cloning, see Table S1	This paper	N/A
Recombinant DNA		
pSIREN-RetroQ-dsRED	Clontech	Cat# 632455
MIGR1-MSCV retro-expression vector	Addgene	Plasmid #27490
Mouse Bach2 sequence-verified cDNA	This Paper	N/A
Mouse Bach2 5' UTR sequence-verified cDNA	This Paper	N/A
Software and Algorithms		

REAGENT or RESOURCE	SOURCE	IDENTIFIER
FlowJo	FlowJo LLC	https://www.flowjo.com/solutions/flowjo/downloads
Graphpad	Prism Graphpad	https://www.graphpad.com/